PERGAMON

International Journal of Solids and Structures 37 (2000) 7809–7820

INTERNATIONAL JOURNAL OF SOLIDS and STRUCTURES

www.elsevier.com/locate/ijsolstr

Numerical analysis of elastic–plastic rotating disks with arbitrary variable thickness and density

L.H. You [a,*], Y.Y. Tang [a], J.J. Zhang [b], C.Y. Zheng [c]

[a] *The College of Mechanical Engineering, Chongqing University, Chongqing City 400045, People's Republic of China*
[b] *The National Centre for Computer Animation, Bournemouth University, Talbot Campus, Poole BH12 5BB, UK*
[c] *Department of Mechanical Engineering, Chongqing Institute of Communications, Chongqing City 400074, People's Republic of China*

Received 11 August 1999

Abstract

A unified numerical method is developed in this article for the analysis of deformations and stresses in elastic–plastic rotating disks with arbitrary cross-sections of continuously variable thickness and arbitrarily variable density made of nonlinear strain-hardening materials. The method is based on a polynomial stress–plastic strain relation, deformation theory in plasticity and Von Mises' yield condition. The governing equation is derived from the basic equations of the rotating disks and solved using the Runge–Kutta algorithm. The proposed method is applied to calculate the deformations and stresses in various rotating disks. These disks include solid disks with constant thickness and constant density, annular disks with constant thickness and constant density, nonlinearly variable thickness and nonlinearly variable density, linearly tapered thickness and linearly variable density, and a combined section of continuously variable thickness and constant density. The computed results are compared to those obtained from the finite element method and the existing approaches. A very good agreement is found between this research and the finite element analysis. Due to the simplicity, effectiveness and efficiency of the proposed method, it is especially suitable for the analysis of various rotating disks.

1. Introduction

Rotating disks have a wide range of applications in engineering, such as high speed gears, fly wheels and turbine rotors. The research on them is always an important topic and their benefits have been included in some books (Timoshenko and Goodier, 1970; Ugural and Fenster, 1987).

Most of the research work are concentrated on the analytical solutions of rotating disks with simple cross-section geometries of constant thickness and specifically variable thickness. The material density of these rotating disks is taken to be either constant or specifically variable. The analytical elasticity solutions of such rotating disks can be found in many books of elasticity. The analytical solution of elastic–perfectly

* Corresponding author. Address: The National Centre for Computer Animation, Bournemouth University, Talbot Campus, Poole BH12 5BB, UK.
E-mail address: lyou@bournemouth.ac.uk (L.H. You).

0020-7683/00/$ - see front matter
PII: S0020-7683(99)00308-X

plastic rotating disks of constant thickness and density was studied by Gamer (1983) using Tresca's yield condition. Gamer (1984a, b) also studied the analytical solutions of such disks with a linear strain-hardening material behaviour using same yield condition. Güven (1992) extended this work to rotating disks of thickness function $h = h_0(r/b)^{-n}$ and density function $\rho = \rho_0(r/b)^m$, and obtained their analytical solution using the same material behaviour and yield condition. As the application of the linear strain-hardening stress–plastic strain relation and Tresca's yield condition can lead to a closed-form solution, they were also applied to study the behaviours of fibrous composites under thermal and thermomechanical loading (You and Long, 1998; You et al., 1999). However, many materials exhibit a nonlinear strain-hardening behaviour. This cannot be described well enough using the linear strain-hardening stress–plastic strain relation. Even for small deformation, as very obvious, nonlinearity occurs in the plastic region close to the yield point of stress–strain curves, it is also valuable to use nonlinear strain-hardening stress–strain or stress–plastic strain relations to approach this nonlinearity. To do this, a polynomial stress–plastic strain relation and a polynomial stress–strain relation have been proposed for the disks of nonlinear strain-hardening materials and were applied to solve the nonlinear strain-hardening elastic–plastic problem of rotating solid disks with a constant thickness and constant density (You et al., 1997; You and Zhang, 1999).

As many rotating components in use have complex cross-sectional geometries, they cannot be dealt with using the existing analytical methods. Numerical methods, such as the finite element method (Zienkiewicz, 1971) and the boundary element method (Banerjee and Butterfield, 1981), can be applied to cope with these rotating components. However, as Sterner et al. (1993) pointed out, these numerical analyses usually require extensive computer resources, are tedious to perform due to extensive meshing requirements and are expensive, making them unsuitable for preliminary design type analysis. Therefore, Sterner et al. (1993) developed a unified numerical method for the elastic analysis of rotating disks with a general, arbitrary configuration based on the repeated application of a truncated Taylor's expansion.

In this article, we will extend the work of Sterner et al. (1993) from elastic analysis to nonlinear strain-hardening elastic–plastic analysis for the rotating disks with arbitrary cross-sections of continuously variable thickness and arbitrarily variable density. In the following, a unified governing equation will be first derived from the basic equations of the rotating disks, deformation theory in plasticity and the proposed stress–strain relationship. Next, Runge–Kutta's algorithm will be introduced to solve the governing equation. Finally, a number of numerical examples are given to demonstrate the validity of the proposed method.

2. Governing equation

As the effect of the thickness variation of rotating disks can be taken into account in their equation of motion, the theory of the disks of variable thickness can give good results as that of the disks of constant thickness as long as they meet the assumption of plane stress. After considering this effect, the equation of motion of rotating disks with variable thickness and variable density can be written as

$$\frac{\mathrm{d}}{\mathrm{d}r}(hr\sigma_{\mathrm{r}}) - h\sigma_\theta + h\rho\omega^2 r^2 = 0, \tag{1}$$

where r is the radial coordinate, σ_{r} and σ_θ are the radial and circumferential stresses, ω, the constant angular velocity, h, the thickness and ρ, the density of the rotating disks which are functions of the radial coordinate r.

The relations between the radial displacement u and the strains are irrespective of the thickness and density of the rotating disks. They can be written as

$$\begin{aligned}\varepsilon_{\mathrm{r}} &= \frac{\mathrm{d}u}{\mathrm{d}r},\\ \varepsilon_{\theta} &= \frac{u}{r},\end{aligned} \tag{2}$$

where ε_{r} is the total radial strain and ε_{θ} the total circumferential strain.

The above geometric relations lead to the following condition of deformation harmony:

$$\frac{\mathrm{d}}{\mathrm{d}r}(r\varepsilon_{\theta}) - \varepsilon_{\mathrm{r}} = 0. \tag{3}$$

The deformation of the rotating disks consists of elastic and plastic components. For the elastic deformation, the relations between the stresses and strains can be described with Hooke's law

$$\begin{aligned}\varepsilon_{\mathrm{r}}^{\mathrm{e}} &= \frac{1}{E}(\sigma_{\mathrm{r}} - v\sigma_{\theta}),\\ \varepsilon_{\theta}^{\mathrm{e}} &= \frac{1}{E}(\sigma_{\theta} - v\sigma_{\mathrm{r}}),\end{aligned} \tag{4}$$

where $\varepsilon_{\mathrm{r}}^{\mathrm{e}}$ and $\varepsilon_{\theta}^{\mathrm{e}}$ are the elastic radial and circumferential strains, E is Young's modulus and v is Poisson's ratio.

For the plastic deformation, the relations between the stresses and plastic strains can be determined according to the deformation theory in plasticity

$$\begin{aligned}\varepsilon_{\mathrm{r}}^{\mathrm{p}} &= \frac{\varepsilon_{\mathrm{e}}^{\mathrm{p}}}{\sigma_{\mathrm{e}}}\left(\sigma_{\mathrm{r}} - \frac{1}{2}\sigma_{\theta}\right),\\ \varepsilon_{\theta}^{\mathrm{p}} &= \frac{\varepsilon_{\mathrm{e}}^{\mathrm{p}}}{\sigma_{\mathrm{e}}}\left(\sigma_{\theta} - \frac{1}{2}\sigma_{\mathrm{r}}\right),\end{aligned} \tag{5}$$

where $\varepsilon_{\mathrm{r}}^{\mathrm{p}}$ and $\varepsilon_{\theta}^{\mathrm{p}}$ are the plastic radial and circumferential strains, $\varepsilon_{\mathrm{e}}^{\mathrm{p}}$ is the equivalent plastic strain and σ_{e} is the equivalent stress

$$\sigma_{\mathrm{e}} = \sqrt{\sigma_{\mathrm{r}}^2 - \sigma_{\mathrm{r}}\sigma_{\theta} + \sigma_{\theta}^2}.$$

The total strains are the sum of the elastic and plastic strains

$$\begin{aligned}\varepsilon_{\mathrm{r}} &= \varepsilon_{\mathrm{r}}^{\mathrm{e}} + \varepsilon_{\mathrm{r}}^{\mathrm{p}},\\ \varepsilon_{\theta} &= \varepsilon_{\theta}^{\mathrm{e}} + \varepsilon_{\theta}^{\mathrm{p}}.\end{aligned} \tag{6}$$

Introducing the stress function ϕ and assuming that the following relations hold between the stresses and the stress function

$$\begin{aligned}\sigma_{\mathrm{r}} &= \frac{1}{hr}\phi,\\ \sigma_{\theta} &= \frac{1}{h}\frac{\mathrm{d}\phi}{\mathrm{d}r} + \rho\omega^2 r^2,\end{aligned} \tag{7}$$

Eq. (1) is satisfied after the substitution of Eq. (7).

Substituting Eq. (7) into Eq. (4), and then substituting Eq. (4) into Eq. (6), one obtains:

$$\begin{aligned}\varepsilon_{\mathrm{r}} &= \frac{1}{E}\left(\frac{1}{hr}\phi - \frac{v}{h}\phi' - v\rho\omega^2 r^2\right) + \varepsilon_{\mathrm{r}}^{\mathrm{p}},\\ \varepsilon_{\theta} &= \frac{1}{E}\left(\frac{1}{h}\phi' - \frac{v}{hr}\phi + \rho\omega^2 r^2\right) + \varepsilon_{\theta}^{\mathrm{p}},\end{aligned} \tag{8}$$

where

$$\phi' = \frac{\mathrm{d}\phi}{\mathrm{d}r}.$$

The substitution of Eq. (8) into Eq. (3) produces

$$r^2\phi'' = -\left(1 - r\frac{h'}{h}\right)r\phi' + \left(1 - vr\frac{h'}{h}\right)\phi - (3+v)h\rho\omega^2 r^3 - h\rho'\omega^2 r^4 - Ehr\left(r\frac{\mathrm{d}\varepsilon_\theta^{\mathrm{p}}}{\mathrm{d}r} + \varepsilon_\theta^{\mathrm{p}} - \varepsilon_r^{\mathrm{p}}\right), \tag{9}$$

where

$$\phi'' = \frac{\mathrm{d}^2\phi}{\mathrm{d}r^2}, \quad h' = \frac{\mathrm{d}h}{\mathrm{d}r}, \quad \rho' = \frac{\mathrm{d}\rho}{\mathrm{d}r}.$$

Adopting the nonlinear strain-hardening material model proposed by You et al. (1997), the stress–strain relationship can be written as:

$$\begin{aligned} &\varepsilon_{\mathrm{e}} = \frac{\sigma_{\mathrm{e}}}{E}, \quad \varepsilon_{\mathrm{e}} \leqslant \varepsilon_0, \\ &\varepsilon_{\mathrm{e}}^{p} = a_1\sigma_{\mathrm{e}}^3 + a_2\sigma_{\mathrm{e}}^5, \quad \varepsilon_{\mathrm{e}} > \varepsilon_0, \end{aligned} \tag{10}$$

where ε_{e} is the equivalent total strain and ε_0, the yield strain.

Substituting the second of Eq. (10) into Eq. (5), the relations between the plastic strains and stresses become:

$$\begin{aligned} \varepsilon_{\mathrm{r}}^{\mathrm{p}} &= (a_1\sigma_{\mathrm{e}}^2 + a_2\sigma_{\mathrm{e}}^4)\left(\sigma_{\mathrm{r}} - \frac{1}{2}\sigma_\theta\right), \\ \varepsilon_\theta^{\mathrm{p}} &= (a_1\sigma_{\mathrm{e}}^2 + a_2\sigma_{\mathrm{e}}^4)\left(\sigma_\theta - \frac{1}{2}\sigma_{\mathrm{r}}\right). \end{aligned} \tag{11}$$

The governing equation in the plastic region of the rotating disks in terms of stresses and stress function can be obtained as follows by substituting Eq. (11) into Eq. (9)

$$\begin{aligned} &\left\{1 + E\left[\frac{1}{2}(a_1 + 2a_2\sigma_{\mathrm{e}}^2)(2\sigma_\theta - \sigma_{\mathrm{r}})^2 + (a_1\sigma_{\mathrm{e}}^2 + a_2\sigma_{\mathrm{e}}^2)\right]\right\}r^2\phi'' \\ &\quad = -\left(1 - r\frac{h'}{h}\right)r\phi' + \left(1 - vr\frac{h'}{h}\right)\phi - (3+v)h\rho\omega^2 r^3 - h\rho'\omega^2 r^4 \\ &\qquad - E\left\{\frac{1}{2}(a_1 + 2a_2\sigma_{\mathrm{e}}^2)(2\sigma_\theta - \sigma_{\mathrm{r}})\left\{(2\sigma_{\mathrm{r}} - \sigma_\theta)\left[r\phi' - \left(1 + r\frac{h'}{h}\right)\phi\right]\right.\right. \\ &\qquad\quad \left.\left. + (2\sigma_\theta - \sigma_{\mathrm{r}})\left(-r^2\frac{h'}{h}\phi' + 2h\rho\omega^2 r^3 + h\rho'\omega^2 r^4\right)\right\} + \left(a_1\sigma_{\mathrm{e}}^2 + a_2\sigma_{\mathrm{e}}^4\right) \\ &\qquad \times\left\{-\left(\frac{1}{2} + r\frac{h'}{h}\right) + \frac{1}{2}\left(+r\frac{h'}{h}\right)\phi + 2h\rho\omega^2 r^3 + h\rho'\omega^2 r^4 + \frac{3}{2}rh(\sigma_\theta - \sigma_{\mathrm{r}})\right\}\right\}. \end{aligned} \tag{12a}$$

In the elastic region, no plastic deformation exists. Therefore, a_1 and a_2 are zero and Eq. (12a) becomes

$$r^2\phi'' = -\left(1 - r\frac{h'}{h}\right)r\phi' + \left(1 - vr\frac{h'}{h}\right)\phi - (3+v)h\rho\omega^2 r^3 - h\rho'\omega^2 r^4. \tag{12b}$$

The values of the stress function ϕ at the elastic–plastic interface radius given by Eqs. (12a) and (12b) are the same. Therefore, the stress function ϕ is continuous at the interface radius. It can be seen from the

continuity of the stress function and Eqs. (7), (4)–(6) and (2) that the continuity conditions of the stresses and displacement at the elastic–plastic interface radius are satisfied.

The boundary conditions for the rotating solid disks are

$$\begin{aligned} &\sigma_{\mathrm{r}} = \sigma_{\theta} \quad \text{at } r = 0, \\ &\sigma_{\mathrm{r}} = 0 \quad \text{at } r = b, \end{aligned} \tag{13}$$

and those for the rotating annular disks are

$$\begin{aligned} &\sigma_{\mathrm{r}} = 0 \quad \text{at } r = a, \\ &\sigma_{\mathrm{r}} = 0 \quad \text{at } r = b, \end{aligned} \tag{14}$$

where a and b are the inner and outer radii of the rotating disks, respectively.

3. Runge–Kutta's algorithm

As shown by Eqs. (12)–(14), the resolution of the elastic–plastic problems of rotating disks with a nonlinear strain-hardening material behaviour is to solve a second-order differential Eq. (12a) under the given boundary conditions (13) or (14). Eq. (12a) can be written in the following general form:

$$\phi'' = f(r, \phi, \phi'). \tag{15}$$

For such a two-point boundary value problem given by Eqs. (15) and (13) or (14), some numerical methods have been developed (see e.g., James et al., 1985). Here we introduce Runge–Kutta's algorithm to solve Eq. (15) subject to the boundary conditions (13) or (14).

Runge–Kutta's iterative formulae for the second-order differential equation are (James et al., 1985)

$$\begin{aligned} \phi'_{i+1} &= \phi'_i + \frac{\Delta r}{6}(K_1 + 2K_2 + 2K_3 + K_4), \\ \phi_{i+1} &= \phi_i + \Delta r\left[\phi'_i + \frac{\Delta r}{6}(K_1 + K_2 + K_3)\right], \end{aligned} \tag{16}$$

where Δr is the increment of the distance along the radius of the rotating disks, and K_1, K_2, K_3 and K_4 can be determined with the following formulae

$$\begin{aligned} K_1 &= f(r_i, \phi_i, \phi'_i), \\ K_2 &= f\left(r_i + \frac{\Delta r}{2}, \phi_i + \frac{\Delta r}{2}\phi'_i, \phi'_i + \frac{\Delta r}{2}K_1\right), \\ K_3 &= f\left(r_i + \frac{\Delta r}{2}, \phi_i + \frac{\Delta r}{2}\phi'_i + \frac{1}{4}\Delta r^2 K_1, \phi'_i + \frac{\Delta r}{2}K_2\right), \\ K_4 &= f\left(r_i + \Delta r, \phi_i + \Delta r\phi'_i + \frac{1}{2}\Delta r^2 K_2, \phi'_i + \Delta r K_3\right). \end{aligned} \tag{17}$$

Once the stress function is obtained, the stresses and displacement in the rotating disks can be calculated using Eqs. (7) and (2).

The numerical simulation starts from the inner boundary, where a trial value of the first-order derivative of the stress function is assumed. Here the stress function at this boundary can be determined by the boundary conditions. Then with a small distance increment Δr, the stress function and its first-order derivative at the new position can be obtained using Eq. (16), and the radial and circumferential stresses are

calculated with Eq. (7). If the equivalent stress at this new position is greater than the yield stress of the disk, Eq. (12a) is used to obtain the second-order derivative of the stress function in the plastic region; otherwise, Eq. (12b) is applied to determine the derivative in the elastic region. The same treatment is repeated from the inner boundary to the outer boundary where the value of the stress function is known. According to the difference between the computed radial stress and the known radial stress at the outer boundary, the initial trial value of the first-order derivative of the stress function at the inner boundary is modified and the next iteration is carried out in the same way. This iterative process is performed until both the boundary conditions are simultaneously satisfied.

4. Numerical simulation

A number of numerical examples of the rotating disks with a nonlinear strain-hardening material behaviour will be given to examine the validity of the proposed method. These examples include: rotating solid disks of constant thickness and constant density, rotating annular disks of constant thickness and constant density, nonlinearly variable thickness $h = h_0(r/b)^{-n}$ and nonlinearly variable density $\rho = \rho_0(r/b)^m$, linearly tapered thickness and linearly variable density, and a combined section with continuously variable thickness and constant density.

The material properties of all the rotating disks to be studied are taken to be: material density $\rho = 7850$ kg/m^3 (for the variable density, this value is the density of the disks at their outer radius), Young's modulus $E = 207$ GPa, Poisson's ratio $v = 0.3$ and yield stress $\sigma_0 = 232.96605$ MPa. The stress–plastic strain relation of the nonlinear strain-hardening rotating disks is taken as

$$\varepsilon_e^p = -9.8652 \times 10^{-11}\sigma_e^3 + 1.8177 \times 10^{-15}\sigma_e^5. \tag{18}$$

In order to make a comparison between the proposed approach and the existing researches, the linear strain-hardening stress–plastic strain relation in the existing research studies is used to approximate Eq. (18) which leads to the following form

$$\sigma_e = 232.96605(1 + 144.3548\varepsilon_e^p). \tag{19}$$

The stress–plastic strain curves from Eqs. (18) and (19) are plotted in Fig. 1 where PSH stands for the nonlinear strain-hardening stress–plastic strain relation, and LSH represents the linear strain-hardening stress–plastic strain relation. It can be seen from the figure that the linear strain-hardening material model cannot describe the nonlinear material behaviour well enough.

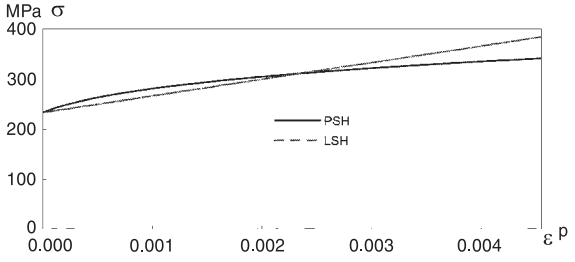

Fig. 1. Stress–plastic strain curves.

4.1. Rotating solid disks of constant thickness and constant density

At first, a rotating solid disk of constant thickness and constant density is studied. The disk has a radius $b = 0.5$ m and rotates at a constant angular velocity $\omega = 650$ rad/s. Three methods, the proposed approach, the existing research (Gamer, 1984a) and the commercially available finite element package of ANSYS revision 5.2, are used to calculate the disk. The obtained results are given in Fig. 2(a)–(e). As shown above, PSH and LSH in these figures and the following figures, respectively, indicate this approach and the existing research studies. FEP denotes the finite element analysis whose stress–plastic strain data are taken from Eq. (18).

The proposed approach gives very agreeable results to the finite element calculation. However, large errors occur between the existing research and the other methods. Compared to the finite element result, the errors of the maximum values of the stresses, plastic strains and radial displacements from this research are 0.03%, 0.51% and 0.24%. However, the existing approach raises these figures to 13.43%, 88.08% and 21.84%. Moreover, the region where the radial plastic strain is zero, given by the existing research, does not exist for the other methods according to Fig. 2(c). Due to this reason, the existing research gives a bigger plastic region (Fig. 2(d)) and bigger radial displacements (Fig. 2(e)) than do the other methods.

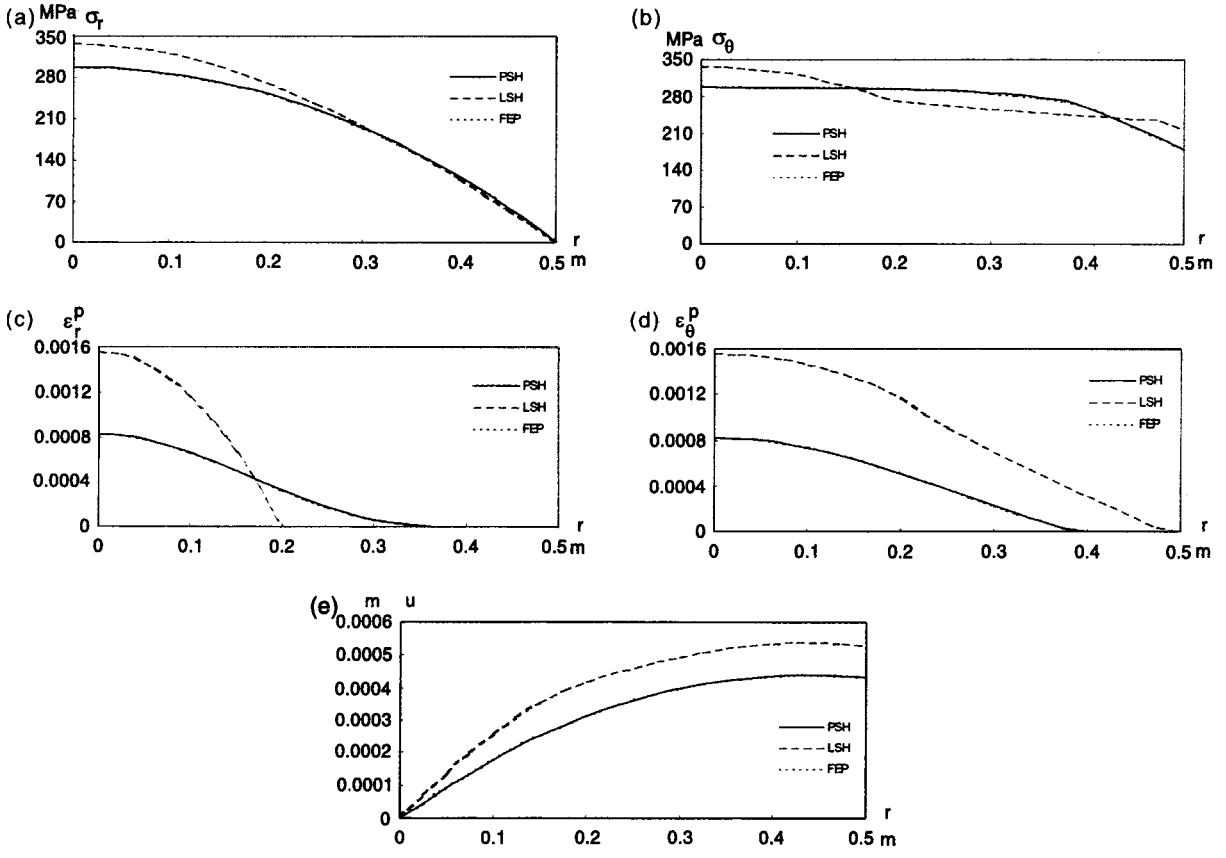

Fig. 2. (a) Radial stresses, (b) circumferential stresses, (c) radial plastic strains, (d) circumferential plastic strains and (e) radial displacements in a solid disk of 0.5 m under 650 rad/s.

4.2. Rotating annular disks of constant thickness and constant density

Taking $n = 0$ in the thickness function $h = h_0(r/b)^{-n}$ and $m = 0$ in the density function $\rho = \rho_0(r/b)^m$ of the rotating annular disk studied by Güven (1992), a rotating annular disk of constant thickness and constant density will be discussed here. The inner and outer radii of the disk are, respectively taken as $a = 0.1$ m and $b = 0.6$ m. The disk rotates at a constant angular velocity $\omega = 190$ rad/s. The calculated stresses, plastic strains and radial displacements are plotted in Fig. 3(a)–(c).

The same conclusions can be drawn from Fig. 3(a)–(c). The proposed approach gives very small errors compared to the finite element calculation. But large errors exist between the existing research and the other methods. The errors of the maximum plastic strain, the circumferential stress and radial displacement at $r = a$ from this research are 1.79%, 0.18% and 0.31%. They become 47.52%, 17.14% and 35.02% for the existing approach. According to the existing research, the radial plastic strain is always zero throughout the entire thickness of the rotating annular disk (see Fig. 3(b)). However, it is not true from the results of the finite element analysis and this research. Similarly, the introduction of zero radial plastic strain makes the disk have a much bigger plastic region (Fig. 3(b)) and bigger radial displacements (Fig. 3(c)).

4.3. Rotating annular disks of nonlinearly variable thickness and nonlinearly variable density

Taking $n = 0.5$ in the variable thickness function $h = h_0(r/b)^{-n}$ and $m = 1$ in the variable density function $\rho = \rho_0(r/b)^m$, a rotating annular disk with such variable thickness and variable density is studied. The inner and outer radii of the disk are taken to be $a = 0.1$ m and $b = 0.5$ m, and the rotating angular velocity is assumed to be $\omega = 730$ rad/s. The results calculated with the above three methods are given in Fig. 4(a)–(c).

For this rotating annular disk, the errors of the maximum plastic strain, the circumferential stress and radial displacement at $r = a$ given by this approach are 1.60%, 0.67% and 0.49%. These numbers go up to 90.88%, 12.35% and 52.20% for the existing research (Güven, 1992). It is clear that for rotating annular disks of variable thickness and variable density, this research can also give very good results, but in the existing approach there still exists big discrepancies.

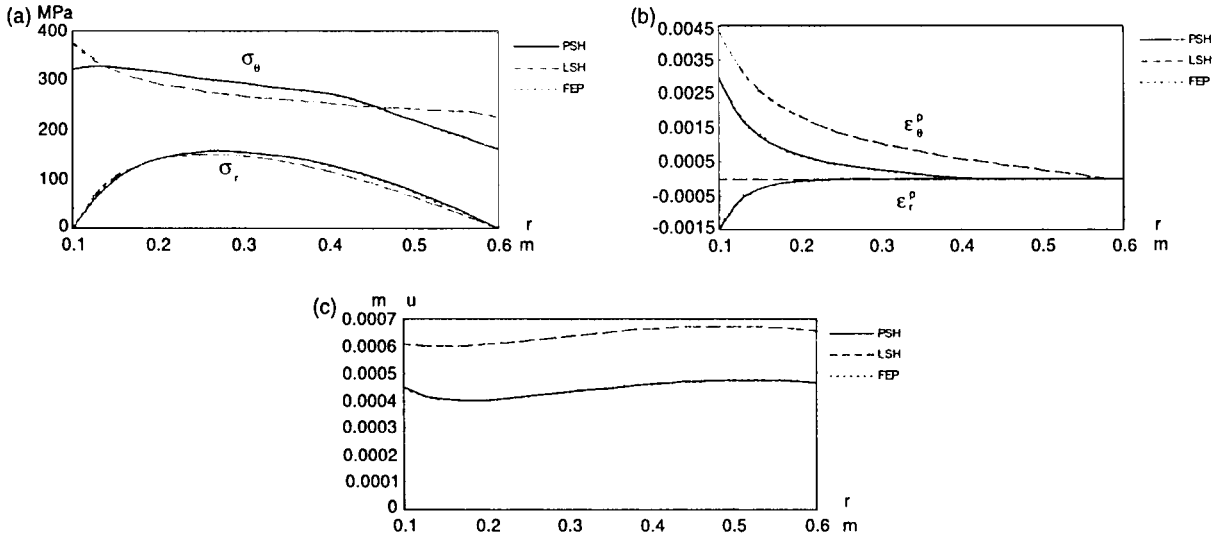

Fig. 3. (a) Stresses, (b) plastic strains and (c) radial displacements in an annular disk with $n = 0$, $m = 0$ under 490 rad/s.

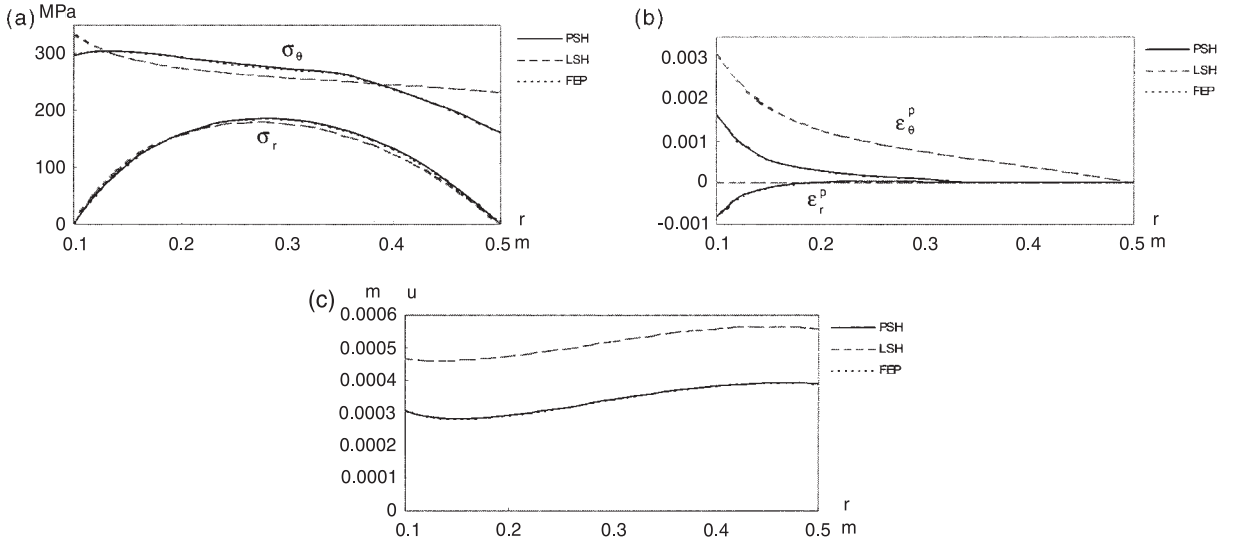

Fig. 4. (a) Stresses in an annular disk with $n = 0.5$, $m = 1$ under 730 rad/s. (b) Plastic strains in an annular disk with $n = 0.5$, $m = 1$ under 730 rad/s. (c) Radial displacements in an annular disk with $n = 0.5$, $m = 1$ under 730 rad/s.

4.4. Rotating annular disks with linearly tapered thickness and linearly variable density

A rotating annular disk with linearly tapered thickness and linearly variable density is investigated. The inner and outer radii of the disk are still taken as $a = 0.1$ m and $b = 0.5$ m. The linearly tapered thickness function and linearly variable density function are

$$h = \frac{(h_b - h_a) \times r + h_a b - h_b a}{b - a}, \tag{20}$$

$$\rho = \frac{1}{2}\rho_0\left(1 + \frac{r}{b}\right), \tag{21}$$

where h_a and h_b are the thickness of the disk at inner and outer radii, respectively, and ρ_0 is the density of the disk at the outer radius $r = b$.

The thickness ratio is assumed to be $h_b/h_a = 2$. The angular velocity of the disk for this case study is $\omega = 500$ rad/s. Since the existing research cannot cope with this rotating annular disk, only the proposed approach and finite element method are applied to analyse the disk. In order to indicate the effect of the material plasticity on the stresses and deformations in the disk, the elastic finite element calculation is also performed. The results obtained with these methods are given in Fig. 5(a) and (b) where PSH and FEP are the same as above, and FEE means the elastic finite element analysis.

Once more, the results given by this research are very close to those from the elastic–plastic finite element analysis. Compared to the elastic–plastic finite element results, the errors of the circumferential stress and radial displacement at $r = a$ are 0.09% and 0.21%, respectively. Without considering the plastic deformation of the disk, the circumferential stresses decrease very quickly in the region outgoing from the inner radius and the maximum circumferential stress always occurs at the inner radius according to the elastic finite element results. Taking the plasticity of the disk into account, the position of maximum circumferential stress is away from the inner radius, and the difference between the circumferential stresses from the elastic and elastic–plastic analyses becomes bigger and bigger as the plastic deformation increases.

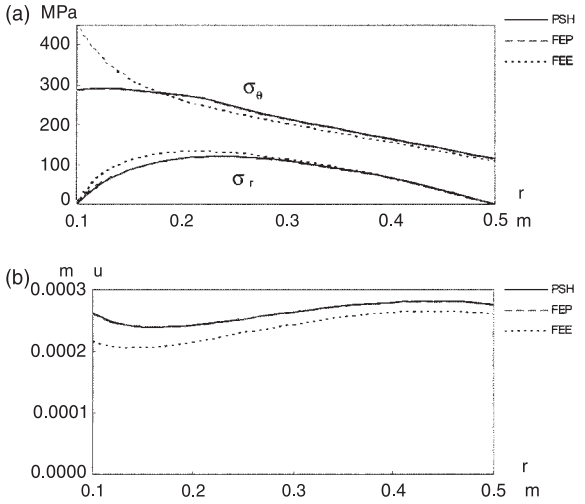

Fig. 5. (a) Stresses in an annular disk with linearly tapered thickness and linearly variable density under 500 rad/s. (b) Radial displacements in an annular disk with linearly tapered thickness and linearly variable density under 500 rad/s.

Moreover, a more and more obvious difference between the elastic and elastic–plastic displacements occurs when moving towards the inner radius.

4.5. Rotating annular disks with a combined section of continuously variable thickness and constant density

The last example is to calculate a rotating annular disk with a combined section of continuously variable thickness and constant density. The calculation of turbine rotors can be simplified as that of such rotating annular disks with a constant angular velocity subjected to a radial stress $\sigma_{r_{external}}$ at the interface between the web and rim of the turbine rotors (Sterner et al., 1993). The cross-section geometry of the rotating annular disk is given in Fig. 6. The boundary conditions (14) for this case study are changed as

$$\begin{aligned} &\sigma_r = 0 \quad \text{at } r = L_0, \\ &\sigma_r = \sigma_{r_{external}} \quad \text{at } r = L_0 + L_h + L_w. \end{aligned} \tag{22}$$

The numerical simulation still starts from the inner boundary. However, as the thickness of the hub in the region of $L_0 \leqslant r \leqslant L_0 + L_h$ is constant, h' is zero in this region. After the values of the stress function and its first- and second-order derivatives at $r = L_0 + L_h$ are obtained, h' is changed to that of the web, and the simulation continues from this position to the outer boundary.

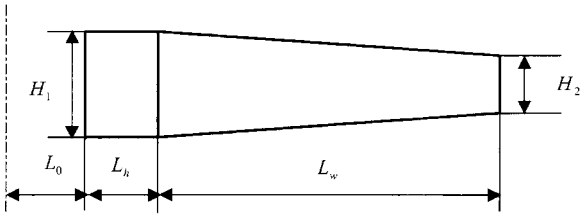

Fig. 6. Cross-section geometry of a rotating annular disk with a combined section.

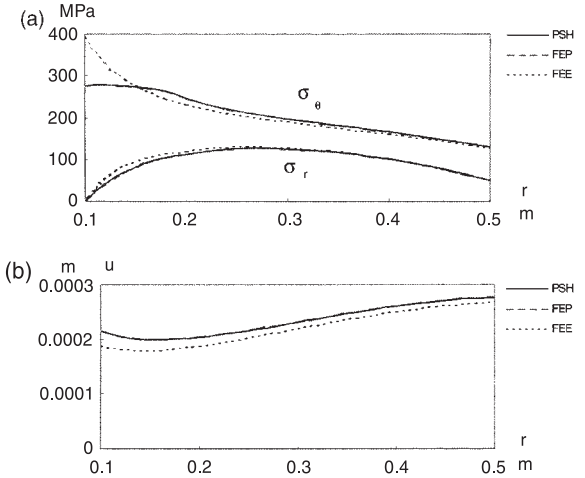

Fig. 7. (a) Stresses in an annular disk with a combined section under 500 rad/s and an externally applied radial stress of 50 MPa. (b) Radial displacements in an annular disk with a combined section under 500 rad/s and an externally applied radial stress of 50 MPa.

In this case study, the geometric data of the disk are $L_0 = 0.1$ m, $L_h = 0.1$ m, $L_w = 0.3$ m and the ratio $H_1/H_2 = 2$. The angular velocity of the disk is taken as $\omega = 500$ rad/s and the externally applied radial stress is 50 MPa. Once again, the existing research cannot deal with the elastic–plastic problem of this disk. For the same reason, this research, elastic–plastic and elastic finite element methods are used to calculate this problem. The calculated results are given in Fig. 7(a) and (b).

Very good results are obtained with the proposed approach. In comparison with the elastic–plastic finite element results, the error of the circumferential stress at inner radius is 0.48% and that of the radial displacement at the same position is 0.51%. The effect of the plastic deformation of the disk on the stresses and radial displacements is the same as that of the rotating annular disk with linearly tapered thickness and linearly variable density.

5. Conclusion

This article presents a unified numerical method for the elastic–plastic calculation of nonlinear strain-hardening rotating disks with a general, arbitrary configuration and arbitrarily variable density. By introducing a suitable stress function, the governing equation was derived from the equilibrium equation, compatibility equation, deformation theory in plasticity, Von Mises' yield condition and the proposed stress–strain relationship of nonlinear strain-hardening. The calculation of the rotating disks was turned into finding the solution of a second-order differential equation under the given conditions at two boundary points. Runge–Kutta's algorithm was introduced to solve the governing equation and a number of numerical examples were studied. The results from this research, the existing approaches and finite element analysis were compared. Obvious errors occur between the existing researches and the other methods. Contrarily, the results given by the proposed approach are in very good agreement with those of the finite element method for all the rotating disks studied. Further, the proposed approach considers the nonlinear strain-hardening behaviour of the disk materials and can cope with the rotating disks with arbitrary cross-sections of continuously variable thickness and arbitrarily variable density, which cannot be dealt with using the existing researches.

References

Banerjee, P.K., Butterfield, R., 1981. Boundary Element Methods in Engineering Science. McGraw-Hill, New York.
Gamer, U., 1983. Tresca's yield condition and the rotating disk. Journal of Applied Mechanics, Transactions of ASME 50, 676–678.
Gamer, U., 1984a. Elastic–plastic deformation of the rotating solid disk. Ingenieur-Archiv 54, 345–354.
Gamer, U., 1984b. The elastic–plastic stress distribution in the rotating annulus and in the annulus under external pressure. Zeitschrift für Angewandte Mathematik und Mechanik 64, T126–T128.
Güven, U., 1992. Elastic–plastic stresses in a rotating annular disk of variable thickness and variable density. International Journal of Mechanical Sciences 34, 133–138.
James, M.L., Smith, G.M., Wolford, J.C., 1985. Applied Numerical Methods for Digital Computation. Harper & Row, New York.
Sterner, S.C., Saigal, S., Kistler, W., Dietrich, D.E., 1993. A unified numerical approach for the analysis of rotating disks including turbine rotors. International Journal of Solids and Structures 31, 269–277.
Timoshenko, S.P., Goodier, J.N., 1970. Theory of Elasticity, Third edn. McGraw-Hill, New York.
Ugural, S.C., Fenster, S.K., 1987. Advanced Strength and Applied Elasticity. Elsevier, New York.
You, L.H., Long, S.Y., Zhang, J.J., 1997. Perturbation solution of rotating solid disks with nonlinear strain-hardening. Mechanics Research Communications 24 (6), 649–658.
You, L.H., Long, S.Y., 1998. Effects of material properties of interfacial layer on stresses in fibrous composites subjected to thermal loading. Composites Part A 29A, 1185–1192.
You, L.H., Long, S.Y., Rohr, L., 1999. Elastic–plastic stress field in a coated continuous fibrous composite subjected to thermo-mechanical loading. Journal of Applied Mechanics, Transactions of ASME 66 (3), 750–757.
You, L.H., Zhang, J.J., 1999. Elastic–plastic stresses in a rotating solid disk. International Journal of Mechanical Sciences 41, 269–282.
Zienkiewicz, O.C., 1971. The Finite Element Method in Engineering Science. McGraw-Hill, London.